PHYSICAL REVIEW B **85**, 220407(R) (2012)

Unusual magnetic properties induced by local structure in a quasi-one-dimensional Ising chain system: α-CoV_2O_6

Bongjae Kim, Beom Hyun Kim, Kyoo Kim, Hong Chul Choi, Sang-Yeon Park, Y. H. Jeong, and B. I. Min*
Department of Physics, Pohang University of Science and Technology, Pohang 790-784, Korea
(Received 18 January 2012; published 28 June 2012)

We have investigated the origins of large orbital magnetic moment (OM) and unique magnetic anisotropy in the quasi-1D magnetic cobaltate, α-CoV_2O_6, employing both the *ab initio* band structure method and the microscopic cluster model calculations. We have found that the peculiar crystal electric field effect in α-CoV_2O_6 combined with the strong spin-orbit coupling induces the unusually large OM and other intriguing magnetic properties of α-CoV_2O_6. The observed 1/3 magnetization plateau in the M-H curve is explained by the spin-flip mechanism based on the MC simulation. Anomalous magnetic entropy behavior is attributed to the strong uniaxial magnetic anisotropy in the quasi-1D Ising chain system.

DOI: 10.1103/PhysRevB.85.220407 PACS number(s): 71.20.−b, 71.70.−d, 75.30.Gw, 75.50.−y

Cobaltate system containing one-dimensional (1D) magnetic chain structure exhibits various interesting features, such as H-field induced spin order-disorder transition,[1,2] magnetic steps in M-H curve,[3–10] large anisotropy,[1,7,11,12] and quantum criticality behavior.[13–15] The underlying physics of the above features, however, has not been well understood yet. CoV_2O_6 (CVO) provides a rare opportunity to explore the roles of various pieces of physics playing out in 1D cobaltate systems because there exist two types of CVO with different local environments, α and γ phase.[7,16–20] α-CVO crystallizes in monoclinic structure,[7,20,21] while γ-CVO in triclinic structure.[17,22] Both α-CVO and γ-CVO are antiferromagnets having ferromagnetically ordered chains, with $T_N = 14$ and 6.3 K, respectively. In both CVOs, edge-shared CoO_6 octahedra form a 1D-like magnetic chain along the b axis, and edge-shared VO_5 square pyramids are located in between the magnetic chains (see Fig. 1). Co is in the divalent state (d^7), while V is in the pentavalent (5+) state with no occupied d electrons (d^0). Hence the general electronic and magnetic properties are determined mostly by Co-3d states.

The saturated magnetic moment of α-CVO was reported to be as large as 4.5 μ_B.[7] Considering the divalent state of Co in α-CVO, the spin magnetic moment would be at most 3.0 μ_B in high-spin (HS) state of Co^{2+}. Then the remaining 1.5 μ_B is thought to come from the orbital magnetic moment (OM). Such large OM of Co is rather exceptional in cobaltates with octahedral coordination. On the contrary, its polymorph γ-CVO has much smaller saturated magnetic moment, 2.9 μ_B. Furthermore, the magnetic anisotropy of α-CVO is distinct from those of other vanadates AV_2O_6 (A = Mn, Cu) including γ-CVO and $CoNb_2O_6$.[16,23] α-CVO has an anisotropic easy axis (c axis in Fig. 1) perpendicular to the chain direction, while all the others have the anisotropic easy axis along the chain direction.

Interestingly, both α-CVO and γ-CVO exhibit 1/3 plateau in the M-H curve. Similar feature of 1/3 plateau has been observed in $Ca_3Co_2O_6$ and its doped relatives,[3,4,6,24,25] and also in cobaltate dihydrates ($CoX_2{\cdot}2H_2O$).[26–28] For those linear chain systems, the plateau behavior is expected to arise from its frustrated equilateral triangular magnetic structure. In CVO, however, such structural frustration is not so obvious since each edge in the triangular lattice has different length. Moreover, anomalous magnetic entropy behavior was observed in CVO.[16–18] The entropy gain above T_N is only 43% of the expected value for HS Co^{2+} ($S = 3/2$). Such intriguing feature of missing entropy was observed ubiquitously in other edge-shared chain-type cobaltate systems,[23,28,29] but the origin has not been clarified yet. Furthermore, magnetodielectric coupling was also found in α phase.[20]

In this Rapid Communication, we have addressed the above mentioned issues of α-CVO : (i) unusually large OM, (ii) unique magnetic anisotropy, (iii) 1/3 plateau in the M-H curve, and (iv) missing magnetic entropy near T_N. We have found that the anomalous features of α-CVO originate from the cooperative action of the crystal electric field (CEF) and the spin-orbit coupling (SOC).

To understand the peculiar features of α-CVO, closer inspection of the highly distorted CoO_6 octahedron in α-CVO is required. Co-O distance along the local z axis is 1.98 Å, which is much shorter than those in the local xy plane, 2.18 and 2.29 Å [see Fig. 1(b)]. In addition, a rectangular distortion is developed in the xy-plane, producing the O-Co-O angle ϕ deviated much from 90° [see Fig. 1(c)]. Accordingly, the CEF becomes much different from the case of ideal octahedron. This is in contrast to the case of γ-CVO, which has almost regular CoO_6 octahedra. In γ-CVO, the maximum difference in Co-O distances of CoO_6 octahedron is less than 5%. Hence, two e_g and three t_{2g} states are split under the octahedral CEF in γ-CVO. The different CEF's produce the fundamental difference of the physical properties between α- and γ-CVO.

To identify the CEF levels of Co octahedron, we first performed the nonmagnetic band calculations for both α-CVO and γ-CVO. For the band calculation, we have employed the full-potential linearized augmented plane-wave (FLAPW) band method[30] implemented in WIEN2K package.[31] Figures 2(a) and 2(b) provide the partial density of states (DOS) of both phases CVO in the generalized gradient approximation (GGA) scheme with the PBEsol functional.[32] Corresponding schematic energy levels are also shown. For α-CVO in Fig. 2(a), three lower states (yz, $x^2 - y^2$, xz) are fully occupied, while the xy state is half filled and the $3z^2 - r^2$ state is almost empty, so as to have d^7 occupation.[38] On the other hand, for γ-CVO, the ordering of the CEF levels is as usual as for the ideal octahedron case. Three lower t_{2g} states (yz, xy,

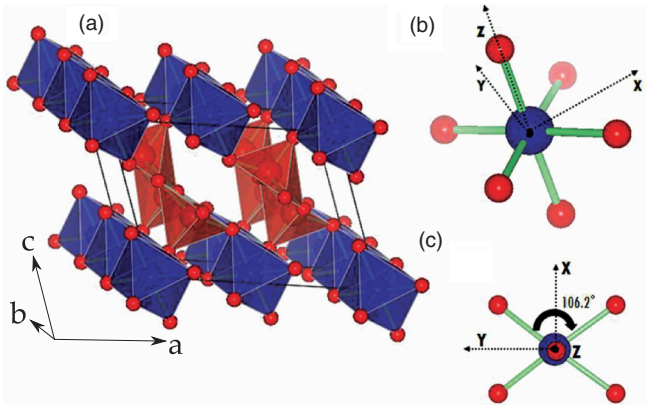

FIG. 1. (Color online) (a) Monoclinic crystal structure of α-CVO. CoO_6 octahedra (blue) form the 1D chain, and VO_5 pyramids (red) sit in between chains. (b) Local axes (x,y,z) of the CoO_6 octahedron. (c) Local axes (x,y) of the CoO_6 octahedron viewed from top. Note that x^2-y^2 state here corresponds to xy state for the normal octahedron. Global axes (a, b, c) almost match the local axes (x,y,z) with only small deviation.

xz) are fully occupied, while the hybridized $x^2-y^2/3z^2-r^2$ state is occupied by one, so as to have d^7 occupation too. The different order of CEF levels originates from the different octahedron shape between two, as mentioned above. In the case of α-CVO, two $e_g(3z^2-r^2$ and $xy)$ states are split greatly due to the shortened Co-O distance along the z axis, and consequently the xy state becomes lowered much closer to t_{2g} states. This distortion is also responsible for making x^2-y^2 the most stable state among the t_{2g} levels. As shown in Fig. 2(a), however, the hybridization with oxygen p states seems to induce the level reordering. In fact, when the hybridization is small, the expected level ordering is brought back, as will be discussed below with Fig. 2(c).

The large OM in α-CVO suggests a strong SOC. Thus we have examined the effects of SOC in α-CVO systematically by performing the spin-polarized band calculations incorporating the SOC. The SOC is included in a second variational scheme (GGA + SO). Also, we consider the orbital-polarization (OP) term (GGA + SO + OP),[33,34] which has been employed to explain the enhanced OM of the cobaltate systems.[35–37] Figures 2(c) and 2(d) provide the partial-DOS (PDOS) obtained in the GGA and the GGA + SO + OP, respectively. In the GGA of Fig. 2(c), the CEF levels in the minority spin PDOS appear to be ordered properly, namely, x^2-y^2 state is the lowest, while $3z^2-r^2$ state is the highest. Also, we note that xy state is separated much from $3z^2-r^2$ state and so becomes close to lower t_{2g} states. In the GGA, Co^{2+} in α-CVO is in the HS state with spin magnetic moment of 2.5 μ_B.

When the SOC is turned on in the GGA + SO, the orbital momentum is induced. Once the CEF in α-CVO pushes down the xy orbital close to the three t_{2g} states, then, due to the SOC, two close pair states (xy and x^2-y^2) and (xz and yz), which are energetically close to each other, can be split in the complex orbital momentum space, as follows: $(d_{xz},d_{yz}) \leftrightarrow (d_1,d_{-1})$; $(d_{xy},d_{x^2-y^2}) \leftrightarrow (d_2,d_{-2})$; $d_{3z^2-r^2} \leftrightarrow d_0$. As shown in the bottom of Fig. 2, this level splitting can provide the maximal OM as large as 3 μ_B for α-CVO. However, the SOC splitting would be incomplete for xy and x^2-y^2, as

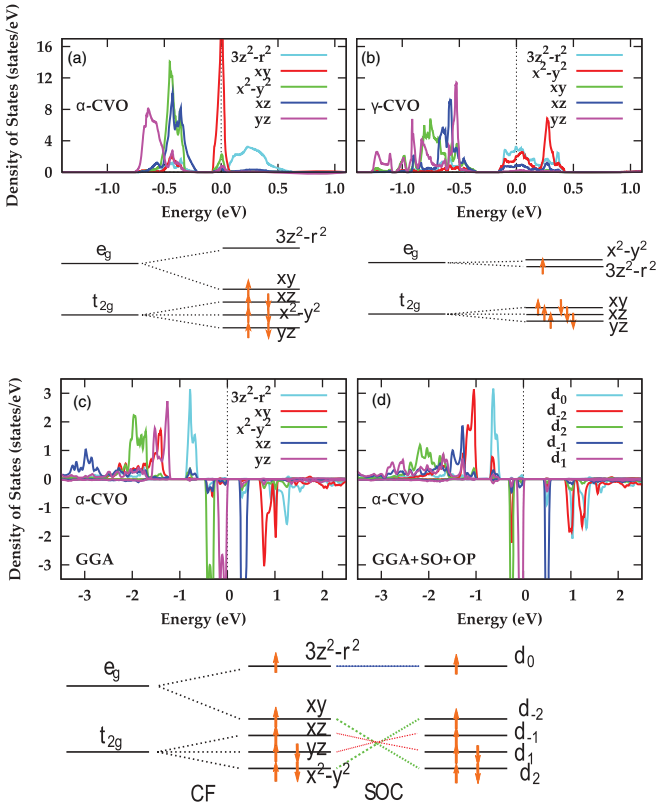

FIG. 2. (Color online) Nonmagnetic PDOSs of Co d for (a) α-CVO and (b) γ-CVO in the GGA. Spin-polarized PDOSs of Co d for α-CVO (c) in the GGA and (d) in the GGA + SOC + OP. Schematic CEF levels of Co are provided below DOSs.

compared to the case of xz and yz, because the former has finite energy separation. The spin and orbital magnetic moments in the GGA + SO are obtained to be 2.46 μ_B and 0.25 μ_B, respectively. The OM is large, but not enough to explain the observed one. So we considered the additional OP term using the GGA + SO + OP scheme. In Fig. 2(d), one can clearly see the level splittings between d_1 and d_{-1} and between d_2 and d_{-2} due to the SOC. This level splitting is reminiscent of that in $Ca_3Co_2O_6$ under the CEF of trigonal prism type, in which the SOC also splits the degenerate states.[12] The OM in the GGA + SO + OP is obtained to be as much as 1.8 μ_B for α-CVO (see Table I).[39]

There exist Co^{2+} systems exhibiting such large orbital magnetic moments.[40–42] Those systems have one hole in the t_{2g} state. In an ideal octahedral CEF, the $10Dq$ separation between the t_{2g} and e_g states is large, and the partially filled t_{2g} levels

TABLE I. Spin and orbital magnetic moments (μ_B) of α- and γ-CVO. The chain is along the b axis for both α-CVO and γ-CVO. The c axis in α-CVO corresponds to the highly contracted octahedron direction.

	α-CVO			γ-CVO		
Magnetic direction	a axis	b axis	c axis	a axis	b axis	c axis
Orbital moment	0.5	0.9	1.8	0.7	0.8	0.3
Spin moment	2.5	2.5	2.4	2.4	2.4	2.4
Total moment	3.0	3.4	4.3	3.1	3.2	2.7

can be described by the pseudo-orbital moment of $\tilde{L} = 1$, by neglecting the effect of higher e_g states. Accordingly, one hole in the minority spin t_{2g} states can produce the OM as large as 1 μ_B. To monitor the CEF effect on the OM, we performed the calculation for hypothetical α-CVO having more ideal CoO_6 octahedra, which are generated lengthening the Co-O distance along the z axis from 1.98 Å to 2.12 Å and reducing ϕ from 106.2° to 95.2°. Then the OM becomes much reduced to 0.88 μ_B, which reflects the important role of the CEF in α-CVO. Interestingly, tetragonally elongated Co-O distance along the z direction, which is the opposite case of α-CVO, is also found to enhance the OM in the Co^{2+} systems.[43]

Now let us analyze the multiplet states of Co^{2+} based on the microscopic Hamiltonian for the distorted CoO_6 octahedron, which includes the intraorbital (U), interorbital (U') Coulomb, exchange (J), pair hopping (J') interactions, and the SOC.[44] In the case of ideal octahedron with O_h symmetry, $^4T_{1g}$ state of $S = 3/2$ and $L = 1$ is stabilized. When the tetragonal distortion with shortened Co-O bond length along the z axis is considered to simulate the case of α-CVO, the ground state becomes ^4E_g. Then the SOC splits the eight degenerate ^4E_g levels into four Kramer's doublets, the lowest two of which are shown in Fig. 4(b). For given Co-O distances, the O-Co-O angle ϕ is found to play a critical role in determining the overall CEF level structure as well as the OM contribution. When ϕ is near 90°, the total magnetic moment obtained in the multiplet calculation is ~4.2 μ_B. As ϕ deviates from 90°, the degeneracy is broken, and the total magnetic moment is reduced to 3.5 μ_B for $\phi = 116°$, which is somewhat different from band calculation result. This suggests that the real ground state of α-CVO cannot be described by a simple cluster model. Still, this model calculation demonstrates the cooperative effect of the CEF and the SOC on the OM.

The cooperative effect of the CEF and the SOC is also responsible for the unique anisotropy of α-CVO. Distinctly from other cobaltates and vanadates, α-CVO has an easy axis along the z axis, which corresponds to the highly contracted Co-O direction of CoO_6 octahedron and is perpendicular to the chain direction. This suggests that the unique anisotropy is related to the CEF of local CoO_6 octahedron, and can be described by the single-ion anisotropy. The *ab initio* band calculation also supports this idea. Calculated OM along each axis in Table I shows that the OM is the largest along the c axis, which corresponds to the anisotropy direction.[7] The magnetocrystalline anisotropy energy (MAE) estimated by using the force theorem[37] also indicates that the c axis is an easy axis with MAE of ~2 meV/f.u. Due to such large MAE, α-CVO has a unique anisotropy that is different from other brannerites, and exhibits strong Ising-type nature. The unique anisotropy in α-CVO was recently claimed to originate from the competition between intrachain and interchain interactions.[19] But it is not likely because the former dominates over the latter, as is discussed below.

In γ-CVO, the size of the OM is reduced with anisotropic easy axis along the chain.[16] As shown in Table I, the OM is the largest along the b axis. In γ-CVO, two e_g and three t_{2g} states remain separated, and so the OM is suppressed, as compared to that of α-CVO. On top of it, the larger bandwidth of γ phase [see Fig. 2(b)] also induces the reduced localized character and the suppressed OM.

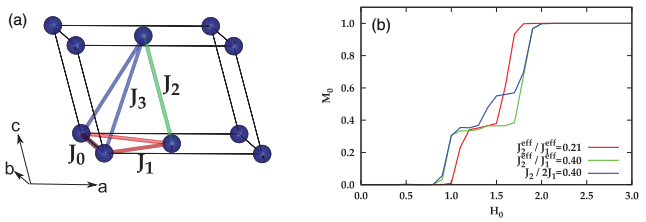

FIG. 3. (Color online) (a) A real 3D lattice structure and interchain interactions. There are twice more spin pairs with J_1 and J_3 than with J_2, and so, in a simple triangular-type model, the effective interactions of $J_1^{\text{eff}} = 2J_1$, $J_2^{\text{eff}} = J_2$, and $J_3^{\text{eff}} = 2J_3$ were assumed. (b) M-H curve from the MC simulation. M_0 is the normalized magnetization and H_0 is in unit of $|J_0|/g\mu_B$. For a triangular-type model, two cases are considered, estimated $J_2^{\text{eff}}/J_1^{\text{eff}} = 0.21$ and larger $J_2^{\text{eff}}/J_1^{\text{eff}} = 0.40$. For a real 3D model, $J_2/2J_1 = 0.40$ is considered.

The 1/3 plateau in the M-H curve is observed both in α- and γ-CVO. The similar behavior in $CoNb_2O_6$ was analyzed in terms of the spin-flip mechanism.[8–11] In $CoNb_2O_6$, its isosceles triangle structure effectively cancels a pair of antiferromagnetic interactions and results in 1/3 plateau behavior through spin-flipping. Similar idea has been adopted for CVO.[20,45] To analyze the spin-flip behavior in more detail, we performed the MC simulation.[46]

We set up the classical spin Hamiltonian of Ising type, $H = \sum_{i,j} J_{ij} S_i S_j$, with J_{ij} being the effective exchange interaction parameter between two Co sites. As described in Fig. 3(a), four different types of interaction parameters are expressed as J_0, J_1, J_2, and J_3. Each parameter is estimated from the total-energy differences among different spin configurations.[47] Interestingly, the effective interaction strengths are estimated to be almost equal ($J_2 = 2J_3$), even though the chain-chain distances are different (6.54 and 6.63 Å). Then, in a simple triangular-type model, the combination with stronger J_1 interaction results in the isosceles-type interaction, and produces the M-H curve in Fig. 3(b), which describes the spin-flip metamagnetism scenario well, as in $CoNb_2O_6$. It is seen that, with increasing $J_2^{\text{eff}}/J_1^{\text{eff}}$, the metamagnetic behavior begins at the smaller fields and covers longer range, but the multistep behavior is well established. Noteworthy is that, if we include

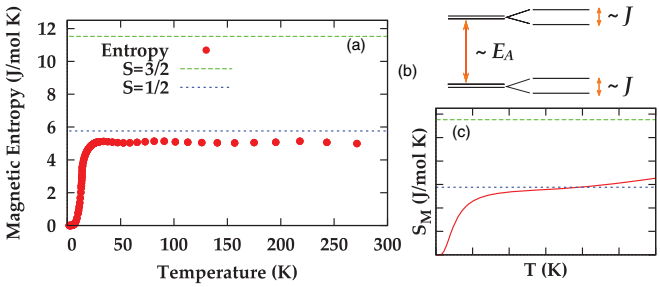

FIG. 4. (Color online) (a) Experimental magnetic entropy S_M of α-CVO obtained by integrating our measured specific heat data.[16] The green and blue dotted horizontal lines represent the entropy values of $S = 1/2$ and $S = 3/2$ spin system, respectively. (b) The schematic energy levels for the lowest two Kramer's doublet of the system. (c) Calculated magnetic entropy S_M. The scales are the same as those of (a).

the effect of different sublattices of a real 3D structure, as in Fig. 3(a), the extra magnetic step, which was not detected in the experiment, is produced [blue line in Fig. 3(b)]. Whether this additional step is due to the oversimplification of overall interactions or it suggests more step behavior as in $Ca_3Co_2O_6$ is of further experimental and theoretical studies.

The magnetic entropy shown in Fig. 4(a) indicates a low-dimensional character of the CVO system. By subtracting the lattice contribution, the magnetic entropy of the α-CVO was obtained by integrating the measured specific heat. The entropy gain above T_N for the HS Co^{2+} ($S = 3/2$) is supposed to be $S_M = R\ln(2S+1) = 11.5$ J/mol K. However, as shown in Fig. 4(a), the measured value corresponds to $S_M = 5$ J/mol K, which is rather close to $S_M = 5.76$ J/mol K for $S = 1/2$. Cobaltate dihydrate, $Co(HCOO)_2{\cdot}2H_2O$, shows a similar behavior, which was once attributed to the partially remained paramagnetic Co^{2+} ions at low temperature.[28] However, this is not the case for α-CVO. Different magnetic energy scales are expected to be the origin of the reduced entropy behavior. The magnetic anisotropy mediated by the intrachain ferromagnetic interaction is much stronger than the interchain spin-flip interaction. Hence the intrachain spin degree of freedom is frozen, and so the spins would act like Ising spins ($S = 1/2$) to manifest the reduced entropy feature.

One can describe the missing entropy behavior on the basis of the microscopic multiplet structure calculation. When the total magnetic moment is 4.2 μ_B, the energy splitting between two lowest doublets is $E_A \approx 25$ meV [see Fig. 4(b)], which is responsible for the strong anisotropic character of the system. Meanwhile, the energy splitting of the doublet due to long-range magnetic order with $T_N = 14$ K can be deduced to be $J = 1.2$ meV, which is responsible for the spin flip. Due to such a big difference between these two energy scales, the contribution of the upper Kramer's doublet to the entropy is almost inert up to room temperature. Indeed, the calculated entropy behavior in Fig. 4(c) is in good agreement with that of the experiment. We think that the seemingly universal feature of missing entropy observed in various edge-shared chain-type cobaltate systems can be understood based on the same analysis.

In conclusion, we have found that the large OM and unique anisotropic behavior of quasi-1D Ising spin system α-CVO arise from the cooperative effects of the CEF of highly distorted CoO_6 octahedron and the SOC. These effects are much suppressed in the polymorph γ-CVO due to its nearly ideal CoO_6 octahedron. The 1/3 plateau behavior in the M-H curve is described by the spin-flip mechanism in the isosceles-type interactions, and the missing entropy feature is explained based on the strong anisotropy of the 1D chain character of α-CVO.

This work was supported by the NRF (Nos. 2009-0079947, 2011-0018037, and 2011-0025237) and by the KISTI supercomputing center (No. KSC-2012-C2-27).

*bimin@postech.ac.kr

[1] Z. He, T. Taniyama, T. Kyômen, and M. Itoh, Phys. Rev. B **72**, 172403 (2005).
[2] S. Kimura, H. Yashiro, K. Okunishi, M. Hagiwara, Z. He, K. Kindo, T. Taniyama, and M. Itoh, Phys. Rev. Lett. **99**, 087602 (2007).
[3] A. Maignan, C. Michel, A. C. Masset, C. Martin, and B. Raveau, Eur. Phys. J. B **15**, 657 (2000).
[4] V. Hardy, M. R. Lees, O. A. Petrenko, D. McK. Paul, D. Flahaut, S. Hébert, and A. Maignan, Phys. Rev. B **70**, 064424 (2004).
[5] V. Hardy, S. Lambert, M. R. Lees, and D. McK. Paul, Phys. Rev. B **68**, 014424 (2003).
[6] Y. B. Kudasov, Phys. Rev. Lett. **96**, 027212 (2006).
[7] Z. He, J.-I. Yamaura, Y. Ueda, and W. Cheng, J. Am. Chem. Soc. **131**, 7554 (2009).
[8] I. Maartense, I. Yaeger, and B. M. Wanklyn, Solid State Commun. **21**, 93 (1977).
[9] S. Mitsuda, S. Kobayashi, K. Aga, H. Katagiri, H. Yoshizawa, M. Ishikawa, K. Miyatani, and K. Kohn, J. Phys. Soc. Jpn. **64**, 2325 (1995).
[10] S. Kobayashi, S. Mitsuda, and K. Prokes, Phys. Rev. B **63**, 024415 (2000).
[11] S. Kobayashi, S. Mitsuda, M. Ishikawa, K. Miyatani, and K. Kohn, Phys. Rev. B **60**, 3331 (1999).
[12] H. Wu, M. W. Haverkort, Z. Hu, D. I. Khomskii, and L. H. Tjeng, Phys. Rev. Lett. **95**, 186401 (2005).
[13] R. Coldea, D. A. Tennant, E. M. Wheeler, E. Wawrzynska, D. Prabhakaran, M. Telling, K. Habicht, P. Smeibidl, and K. Kiefer, Science **327**, 177 (2010).
[14] S. Lee, R. K. Kaul, and L. Balents, Nat. Phys. **6**, 702 (2010).
[15] S. Sachdev and B. Keimer, Phys. Today **64**, 29 (2011).
[16] S. Y. Park *et al.* (unpublished).
[17] S. A. J. Kimber, D. N. Argyriou, and J. P. Attfield, arXiv:0804.2966.
[18] S. A. J. Kimber, H. Mutka, T. Chatterji, T. Hofmann, P. F. Henry, H. N. Bordallo, D. N. Argyriou, and J. P. Attfield, Phys. Rev. B **84**, 104425 (2011).
[19] M. Lenertz, J. Alaria, D. Stoeffler, S. Colis, and A. Dinia, J. Phys. Chem. C **115**, 17190 (2011).
[20] K. Singh, A. Maignan, D. Pelloquin, O. Perez, and Ch. Simon, J. Mater. Chem. **22**, 6436 (2012).
[21] B. Jasper-Toennie and H. Müeller-Buschbaum, Z. Anorg. Allg. Chem. **508**, 7 (1984).
[22] H. K. Müller-Buschbaum and M. Kobel, Zeit. Ang. Allg. Chem. **596**, 23 (1991).
[23] T. Hanawa, K. Shinkawa, M. Ishikawa, K. Miyatani, K. Saito, and K. Kohn, J. Phys. Soc. Jpn. **63**, 2706 (1994).
[24] S. Rayaprol, K. Sengupta, and E. V. Sampathkumaran, Solid State Commun. **128**, 79 (2003).
[25] Y. J. Choi, H. T. Yi, S. Lee, Q. Huang, V. Kiryukhin, and S. W. Cheong, Phys. Rev. Lett. **100**, 047601 (2008).
[26] H. Kobayashi and T. Haseda, J. Phys. Soc. Jpn. **19**, 765 (1964).
[27] T. Shinoda, H. Chihara, and S. Seki, J. Phys. Soc. Jpn. **19**, 1637 (1964).
[28] M. Matsuura, H. W. J. Blöte, and W. J. Huiskamp, Physica **50**, 444 (1970).
[29] Z. He, D. Fu, T. Kyômen, T. Taniyama, and M. Itoh, Chem. Mater. **17**, 2924 (2005).

[30]H. J. F. Jansen and A. J. Freeman, Phys. Rev. B **30**, 561 (1984).

[31]P. Blaha *et al.*, WIEN2K, Karlheinz Schwarz, Techn. Universität Wien, Austria, 2001.

[32]J. P. Perdew, A. Ruzsinszky, G. I. Csonka, O. A. Vydrov, G. E. Scuseria, L. A. Constantin, X. Zhou, and K. Burke, Phys. Rev. Lett. **100**, 136406 (2008).

[33]M. S. S. Brooks, Physica B **130**, 6 (1985).

[34]O. Eriksson, B. Johansson, and M. S. S. Brooks, J. Phys.: Condens. Matter **1**, 4005 (1989).

[35]M. R. Norman, Phys. Rev. Lett. **64**, 1162 (1990).

[36]P. Ravindran, R. Vidya, O. Eriksson, and H. Fjellvåg, Adv. Mater. **20**, 1353 (2008).

[37]G. H. O. Daalderop, P. J. Kelly, and M. F. H. Schuurmans, Phys. Rev. B **53**, 14415 (1996).

[38]For α-CVO, $x^2 - y^2$ and xy states are interchanged since local xy axis are rotated by 45° from Co-O axis [see Fig. 1(c)]. γ-CVO follows the normal convention.

[39]We have also performed the hybrid-functional calculation with PBE0 and PBEsol0, and obtained the OM of 2.3 μ_B.

[40]N. Hollmann, M. W. Haverkort, M. Cwik, M. Benomar, M. Reuther, A. Tanaka, and T. Lorenz, New J. Phys. **10**, 023018 (2008).

[41]T. Burnus, Z. Hu, H. H. Hsieh, V. L. J. Joly, P. A. Joy, M. W. Haverkort, H. Wu, A. Tanaka, H.-J. Lin, C. T. Chen, and L. H. Tjeng, Phys. Rev. B **77**, 125124 (2008).

[42]S. I. Csiszar, M. W. Haverkort, Z. Hu, A. Tanaka, H. H. Hsieh, H.-J. Lin, C. T. Chen, T. Hibma, and L. H. Tjeng, Phys. Rev. Lett. **95**, 187205 (2005).

[43]C. F. Smura, D. R. Parker, M. Zbiri, M. R. Johnson, Z. A. Gál, and S. J. Clarke, J. Am. Chem. Soc. **133**, 2691 (2011).

[44]We set $U = U' + 2J$ and $J = J'$ with $U = 8.0$ eV, $J = 1.0$ eV, and the SOC $\lambda = 0.0638$ eV.

[45]X. Yao, J. Phys. Chem. A **116**, 2278 (2012). The MC calculation was performed in a simple 2D triangular lattice with consideration of chain-chain interactions only.

[46]N. Metropolis, A. W. Rosenbluth, M. N. Rosenbluth, A. H. Teller, and E. Teller, J. Chem. Phys. **21**, 1087 (1953). The MC simulation is performed on $20 \times 10 \times 20$ lattice with the periodic boundary condition for two sublattices. By using the standard Metropolis algorithm, we have spanned 30 000 thermalization and 30 000 calculation steps at each field.

[47]We obtained relative ratios of $J_2^{\text{eff}}/J_1^{\text{eff}} = 0.21$.